https://doi.org/10.5194/hess-2021-590
Preprint. Discussion started: 1 December 2021

Hydrology and Earth System Sciences
Discussions

Estimation Standard And Seeded Pan Evaporation Using Modelling Approach

Brigitta Simon-Gáspár[1], Gábor Soós[1], Angela Anda[1]

[1]Hungarian University of Agriculture and Life Sciences, Georgikon Campus, P. O. Box 71 Keszthely, H-8361 Hungary

Correspondence to: Brigitta Simon-Gáspár (simon.gaspar.brigitta@uni-mate.hu)

Abstract. Evaporation is an important meteorological variable that has also a great impact on water management. In this study, FAO-56 Penman-Monteith equation (FAO56-PM), multiple stepwise regression (MLR) and Kohonen self-organizing map (K-SOM) techniques were used for the estimation of daily pan evaporation (E_p) in three treatments, where C was the standard class A pan with top water, S was A pan with sediment covered bottom, and SM was class A pan containing submerged macrophytes (*Myriophyllum sipctatum*., *Potamogeton perfoliatus*, and *Najas marina*), in an six-season experiment. The modelling approach included six measured meteorological variables; daily mean air temperatures (T_a), maximum and minimum air temperatures, global radiation (R_s), relative humidity (RH), and wind speed (u) in the 2015-2020 growing seasons (from June to September), at Keszthely, Hungary. Average E_p varied from 0.6 to 6.9 mm d^{-1} for C, 0.7 to 7.9 mm d^{-1} for S, whereas from 0.9 to 8.2 mm d^{-1} for SM during the growing seasons studied. Correlation analysis and K-SOM visual representation revealed that T_a and R_s had stronger positive correlation, while RH had a negative correlation with the E_p of C, S and SM. Performances of the different models were compared using statistical indices, which included the root mean square error (RMSE), mean absolute error (MAE), scatter index (SI) and Nash-Sutcliffe efficiency (NSE). The results showed that the MLR method provided close compliance with the observed pan evaporation values, but the K-SOM method gave better estimates than the other methods. Overall, K-SOM has high accuracy and huge potential for E_p estimation for water bodies where freshwater submerged macrophytes are present.

1 Introduction

Open water evaporation is one of the paramount elements of the hydrological cycle (Brutsaert, 1982). Evaporation losses from various surfaces appear to be increasing in recent decades (Mbangiwa et al., 2019). Due to climate change, it is also extremely important to determine evaporation as accurately as possible (Fournier et al., 2021), for which both direct and indirect methods are available. As a direct method, the evaporation pans (primarily the class A pan proposed by the World Meteorological Organization, WMO) are used extensively throughout the world to measure open water evaporation and to estimate reference evapotranspiration (Rahimikhoob, 2009). Measurements of pan evaporation may be spatially and temporally limited (Jensen et el., 1990; Rahimikhoob, 2009), like in case of maintenance problems which can affect the accuracy of evaporation measurements, e.g., most often turbidity of water, watering of birds or other animals (Tabari et al., 2010).

https://doi.org/10.5194/hess-2021-590
Preprint. Discussion started: 1 December 2021


Hydrology and Earth System Sciences
Discussions

To indirectly determine evaporation, several methods can be used: empirical equations are applied that estimate evaporation based on meteorological variables (air temperature, T_a, relative humidity, RH, global radiation, R_s), or transfer and water budget methods (Burman, 1976). The most widely used empirical formula is a FAO-56 Penman–Monteith equation (FAO56-PM) (Allen et al., 1998), which is the standard method for computation of daily reference evapotranspiration. However, measuring meteorological variables requires sophisticated instruments, which can often be challenging (Arunkumar and Jothiprakash, 2013). The amount of required data and the difficulty of the estimation of the unknown meteorological elements may be additional problems (Sanikhani et al., 2015; Khatibi, Ghorbani, Naghshara et al., 2020). Therefore, there is a need for alternative methods that are simple and effective, require fewer inputs and are also able to solve problems which are difficult to formalize (Sudheer et al., 2003).

A promising tool that can be used to estimate E_p and is a suitable alternative to the empirical models is the different neural networks (Kim et al., 2015), thus the neural networks are increasingly used in evaporation and evapotranspiration estimation (Kumar et al., 2002; Keskin and Terzi 2006; Rahimikhoob, 2009). The machine learning techniques can map high dimensional data to a low dimensional space and show some similar properties based on internal data relationships (Pearce et al., 2011; Zelazny et al., 2011). In recent years, machine learning techniques have been broadly employed in hydrological and environmental models, including to forecast evaporation (Wu et al., 2020). Numerous results in the literature indicate that machine learning algorithms such as artificial neural network (ANN), M5 model tree (M5T), support vector machines (SVM), multivariate adaptive regression splines (MARS), gradient boosting with categorical features support (CatBoost), random forest (RF) perform excellently in predicting pan evaporation as well (Dong et al., 2021). The unsupervised NNs, including Kohonen Self Organizing Maps (K-SOM), has several advantages (Kohonen, 1982). The essence of this method is to group the large-dimensional array of the input layer into a 2-dimensional array in the output layer, so that all variables of the input vectors can be found in each node of the output layer (Adeloye et al., 2011). Another advantage of K-SOM over traditional models is that it also has visualization abilities (Hadjisolomou et al., 2018).

Whether it is an empirical formula or NN, the values of the model are compared to the observed values. Evaporation of open water surfaces is usually measured by means of pans endowed with unrealistic properties. These pans are filled with clean tap water and the evaporated water is also replaced with tap water. The literature data therefore refer to these pans filled with clean water. In nature, however, there may also be submerged macrophyte living in the open water. These plants are primary producers in lake ecosystems (Kimmel and Groeger, 1984; Zhang et al., 2017), thus, their presence is essential and affects the water quality (Yan et al., 2019). Furthermore, the species that are rooted in the sediment can stabilize the sediment by inhibiting its resuspension (Madsen and Cedergreen, 2002; Vymazal, 2013). T_a is an important factor in crop appearance and related variations in the duration of seasons as well as growth and development of the submerged macrophyte (Barko et al., 1982). Changes in the T_a regime of a water body had been reported to result in alterations of macrophyte community composition (Barko et al., 1982), which may affect the temporal appearance and spatial distribution of macrophytes in the future. As a result, due to global climate change, it is of paramount importance to examine submerged macrophytes in all aspects, including their effect on evaporation.

https://doi.org/10.5194/hess-2021-590
Preprint. Discussion started: 1 December 2021

Hydrology and Earth System Sciences
Discussions

Since there is little information in the literature on how submersed macrophytes affect the evaporation of a lake, one of the aims of this study was to investigate the effect of littoral sediment and macrophytes on E_p. At the study site, in Hungary, submerged macrophytes colonize in lakes in the summer season (from June to September). Lake Balaton is the largest shallow freshwater lake in Central Europe with surface area of 596 km^2 (Figure 1). The three most dominant submerged macrophytes in the Lake Balaton are *Potamogeton perfoliatus*, *Myriophyllum spicatum* and *Najas marina*, therefore, it was appropriate to include these three species in the study.

The second main aim of this paper was to estimate daily E_p using FAO-56 Penman-Monteith (FAO56-PM), Kohonen self-organization map (K-SOM) and multiple stepwise linear regression (MLR) methods in class A pan with different ingredients, sediments and macrophytes. The current study differs from previous evaporation estimates by using NNs even with those pans containing sediments and submerged macrophytes. Their evaporation will be treated directly by K-SOM, in which the modelling is more than the simple E_p of a Class A pan filled with clean tap water.

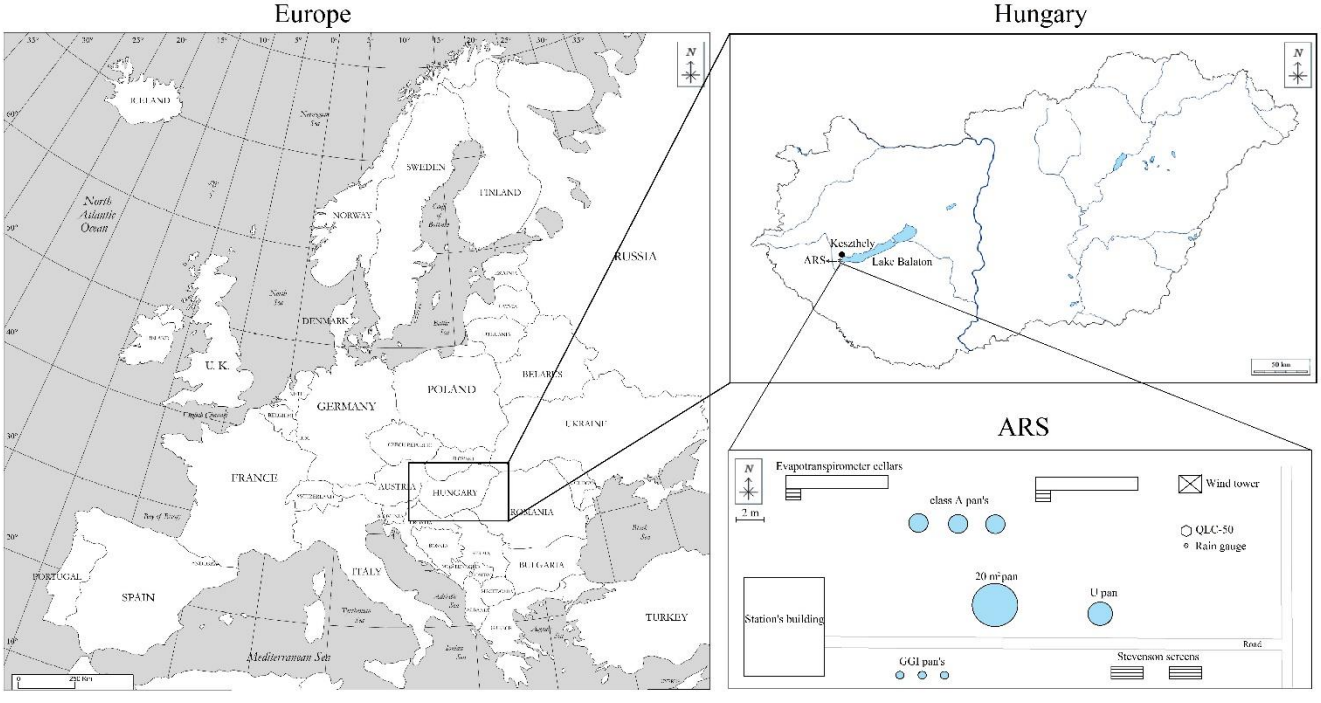

Figure 1: Location map of the study area with Agrometeorological Research Station (ARS) at Keszthely, Hungary (from http://alabamamaps.ua.edu).

https://doi.org/10.5194/hess-2021-590
Preprint. Discussion started: 1 December 2021

Hydrology and Earth System Sciences
Discussions

2 Materials and methods

2.1 Case study and data description

The climate of the region is mild continental (Cfb) with warm, dry summers and fairly cold winters according to the Köppen-Geiger classification (Kottek, Grieser, Beck, Rudolf and Rubel, 2006). Months included in the study (from June to September). Meteorological variables were recorded by a QLC-50 climate station (Vaisala, Helsinki, Finland) fitted with a CM-3 pyranometer (Kipp & Zonen Corp., Delft, the Netherlands) located at Keszthely Agrometeorological Research Station (ARS) (latitude: 46°44′N, longitude: 17°14′E, elevation: 124 m above sea level) between 2015-2020. The ARS is placed on the area of the Hungarian University of Agriculture and Life Sciences. With the exception of wind speed, meteorological data of T_a, RH, R_s, daily maximum temperature (T_{max}), daily minimum temperature (T_{min}) and precipitation (P)were measured at 2 m above the ground surface. The height of windspeed (u) measurements was 10.5 m. The daily mean values of meteorological variables were calculated as average of 10 minutes observations of a 24-hour period.

In this study, class A evaporation pans were used to determine daily evaporation (E_p). The class A pans were 1.21 m in diameter and 0.25 m in height located on an elevated (~0.15 m) wooden grid, with a water surface area of ~1.15 m^2. The daily rate of E_p was calculated from the difference in water level for two consecutive days, considering any precipitation that may have fallen into the pans. The daily water loss was measured every morning at 7.00 am LMT.

In the ARS area 3 class A pans were placed, 5 meters apart (Figure 2). A class A pan was recommended by the WMO to be used as a standard treatment (control, C). Two class A pans were covered on the bottom with sediment to a thickness of 0.002 m (S). Submerged, freshwater aquatic macrophytes (*Myriophyllum sipctatum*., *Potamogeton perfoliatus*, and *Najas marina*) were planted in three class A pans with sediment-covered bottom (Anda et al., 2016; Anda et al., 2018). Due to the development of submersed macrophytes, Class A pans were operational from June to September in the growing season 2015-2020.

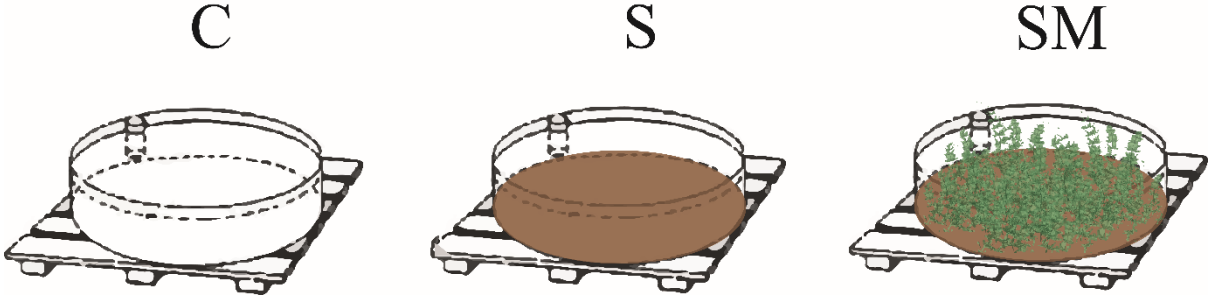

Figure 2: Class A pans with different treatments: C, S and SM denote ‘‘empty”, sediment-covered and macrophyte-planted class A pans in the middle of the meteorological garden.

2.2 Multiple stepwise regression (MLR)

The regression models are important tools for investigating relations between dependent and independent data (Razi and Athappilly, 2005), which method has been used for a long time in the investigation of meteorological variables. Evaporation can be modelled by multiple linear regressions using different meteorological variables (e.g., Ta, RH, u) (Almedeij, 2012).

https://doi.org/10.5194/hess-2021-590
Preprint. Discussion started: 1 December 2021


Hydrology and Earth System Sciences
Discussions

105 The MLR can be expressed by the following equation:

$$y = b_0 + b_1 x_1 + \cdots + b_k x_k + a\,, \quad (1)$$

where b_0, b_1 … and b_k are fitting constant, x_1… and x_k represent the observed meteorological variables and a is a random error term. The a is remaining effects on estimated E_p (y) of variables not explicitly included in the model (Patle et al., 2020). The dependent variable, y was E_p.

110 **2.3 FAO-56 Penman-Monteith (FAO56-PM) method**

The reference evapotranspiration ET_0 was estimated by the WMO standardized FAO-56 Penman-Monteith method (Allen et al., 1998; Allen et al., 2005) the at a daily step for short reference crops (clipped grass of 12 cm) as followed:

$$ET_0 = \frac{0.408\Delta(R_n - G) + \gamma \frac{900}{T_a + 273} u(e_s - e_a)}{\Delta + \gamma(1 + 0.34u)}, \quad (2)$$

where R_n is net radiation [MJ m^{-2} d^{-1}], G is the soil heat flux density [MJ m^{-2} d^{-1}], T_a is the mean daily air temperature at 2 m
115 height [°C], u is wind speed [m s^{-1}] at 2 m height, e_s is the saturation vapor pressure [kPa], e_a is the actual vapor pressure [kPa], Δ is the slope of the vapor pressure curve [kPa $°C^{-1}$], γ is a psychrometric constant [kPa $°C^{-1}$], and 0.408 is a conversion factor from MJ m^{-2} d^{-1} to equivalent evaporation in mm d^{-1}.

2.4 Kohonen self-organization map (K-SOM)

The K-SOM is a nonlinear mapping technique, which identifies groups of similarity in data sets without normal distribution
120 assumption (Kohonen, 1982). SOM is a powerful and effective tool for complex data analyses such as data mining, estimation, and prediction. Using SOM, informative reference vectors are obtained via iterative updates under three main successive procedures: competition with nodes (1), selection of a winner node (2) and updating of the reference vector (3) (Yu et al., 2018). Every node has its vector adjusted according to sequential algorithm with the Gaussian neighbourhood function. The SOM consists of an input layer and an output layer (Park et al., 2006), where the output layer consists of so-called neurons,
125 which are usually located in a hexagonal grid and are fully interconnected (Peeters et al., 2007). A schematic illustration of K-SOM is presented in Figure 3.

https://doi.org/10.5194/hess-2021-590
Preprint. Discussion started: 1 December 2021

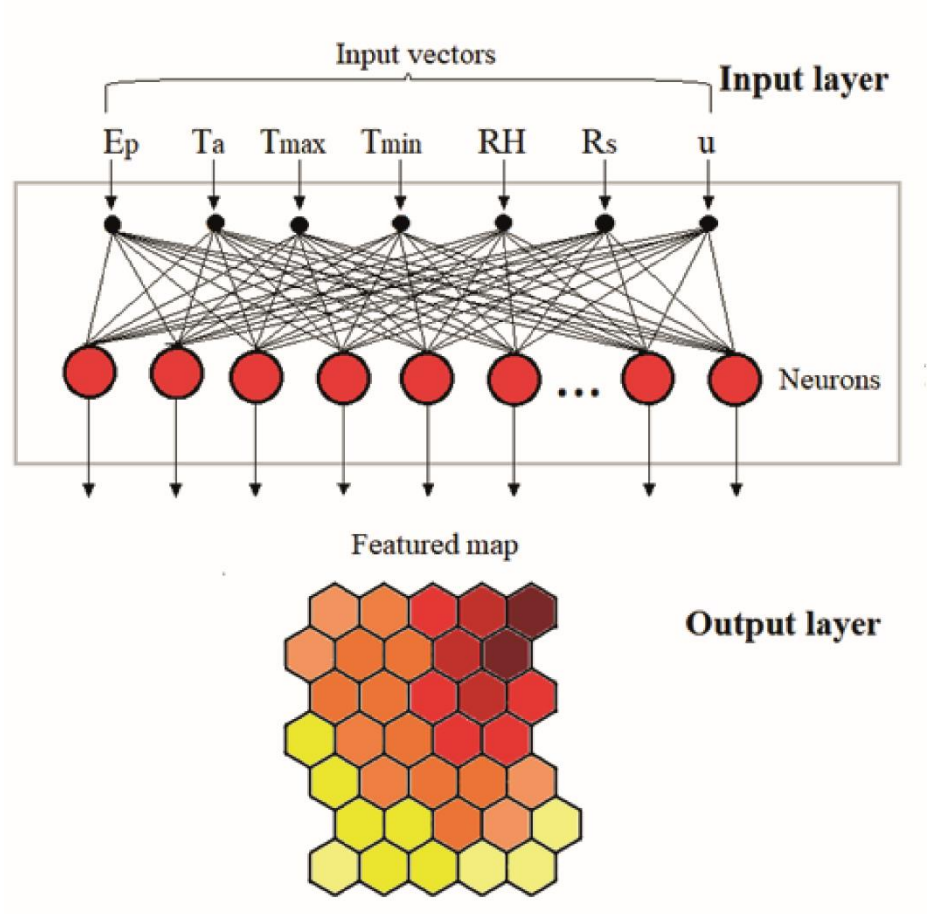

Figure 3: Illustration of the winning node and its neighbourhood in the Kohonen self-organizing map (K-SOM).

The importance of K-SOM in the field of environmental science lies in the fact that SOMs can be used for prediction and correlation analysis, mostly with visual representation (Barreto and Pérez-Uribe, 2007). An outstanding element of this is that K-SOM finds statistically significant dependencies among the variables in a multidimensional data sample. In the case where two variables are highly correlated, K-SOM produces two similar component planes (Barreto and Pérez-Uribe, 2007).

2.5 Statistics and performance evaluation criteria

The Shapiro–Wilk test was used as a statistical test for normality, with a chosen alpha value of 0.05 ($p<0.05$). Two-way analysis of variance (ANOVA) with Tukey's HSD test was performed to examine the impacts of treatments C, S and SM on class A pan E_p. The impact of meteorological elements on E_p of C, S and SM treatments, Pearson's correlation analysis was used. This, as well as the MLR, was carried out with SPSS Statistics software. In this study, the K-SOM algorithm was executed

https://doi.org/10.5194/hess-2021-590
Preprint. Discussion started: 1 December 2021


Hydrology and Earth System Sciences
Discussions

using MATLAB 2019b software. To train and test the models, 50% of the data (2015–2017) and 50% (2018–2020) were used, respectively.

Performance of the proposed models is evaluated by computing statistical indices, such as root mean square error (RMSE), mean absolute error (MAE), scatter index (SI) and Nash-Sutcliffe efficiency (NSE) between observed and estimated values of E_p for the data sets considered. The RMSE range is zero to infinity ($0 < RMSE < \infty$); the lower the RMSE, the better the model's performance. The RMSE is proportional to the observed mean, as a result SI (Shiri and Kişi, 2011) forms a good non-dimensional error measure. NSE (Nash and Sutcliffe 1970; ASCE 1993) compares the congruence between the observed and predicted data. A high value of NSE (NSE ≤ 1) indicates high efficiency of the model (Duan et al., 2016; Li and Liu, 2020). These evaluation criteria calculate as following equations:

$$RMSE = \sqrt{\frac{\sum_{i=1}^{n}(E_{p_{obs,i}} - E_{p_{est,i}})^2}{n}}, \quad (3)$$

$$MAE = \frac{\sum_{i=1}^{n}\left|E_{p_{est,i}} - E_{p_{obs,i}}\right|}{n}, \quad (4)$$

$$NSE = 1 - \frac{\sum_{i=1}^{n}(E_{p_{obs,i}} - E_{p_{est,i}})^2}{\sum_{i=1}^{n}(E_{p_{est,i}} - E_{p_{est,m}})^2}, \quad (5)$$

$$SI = \sqrt{\frac{\sum_{i=1}^{N}\left[\left(E_{p_{est,i}} - E_{p_{est,m}}\right) - \left(E_{p_{obs,i}} - E_{p_{obs,m}}\right)\right]}{\sum_{i=1}^{N} E_{p_{obs,i}}^2}}, \quad (6)$$

where $E_{p\ obs,i}$, $E_{p\ est,i}$ observed and estimated pan evaporation values on the i^{th} day, $E_{p\ obs,m}$ and $E_{p\ est,m}$ is the mean value of $E_{p\ obs,i}$ and $E_{p\ est,I}$, respectively. The total number of testing patterns is denoted by n and i represent the number of particular instances of the testing pattern.

3 Results

3.1 Meteorological variables and pan evaporation

The long-term (1971–2000) growing season's average T_a at Keszthely is 18.8 °C, the hottest month is July with a mean monthly T_a of 20.5 °C, while the coolest month is September (15.7 °C). In the study period, the seasonal mean T_a were 5.5-15.7% higher than the 30-year average. The climate of Keszthely is characterized by highly variable and irregular P with a long-term seasonal total of 274.3 mm from June to September. Monthly seasonal mean precipitation sums varied from 78.5 mm (June) to 57.1 mm (September). Out of six investigated seasons, 2015 and 2019 were characteristically arid with 27.6% and 26.4% less seasonal total P, respectively, compared to the 30-year average. In the other study seasons, there were 4.7-30.7% more P (data not shown) than that of the climate norm.

Figure 4 displays the meteorological variables and observed daily E_p in different pan treatments determined in a box-and-whisker plot between growing season 2015-2020, indicating minimum, first quartile, median, third quartile, and maximum

https://doi.org/10.5194/hess-2021-590
Preprint. Discussion started: 1 December 2021

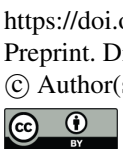

Hydrology and Earth System Sciences
Discussions

values. An increasing trend was observed in the T_{min} with an increment of 9.6% while the T_{max} exhibited an unchanged trend over the studied growing seasons. RH and R_s displays a regular pattern during the 6 growing seasons. In terms of averages, an unchanged trend is observed in u with an irregular pattern.

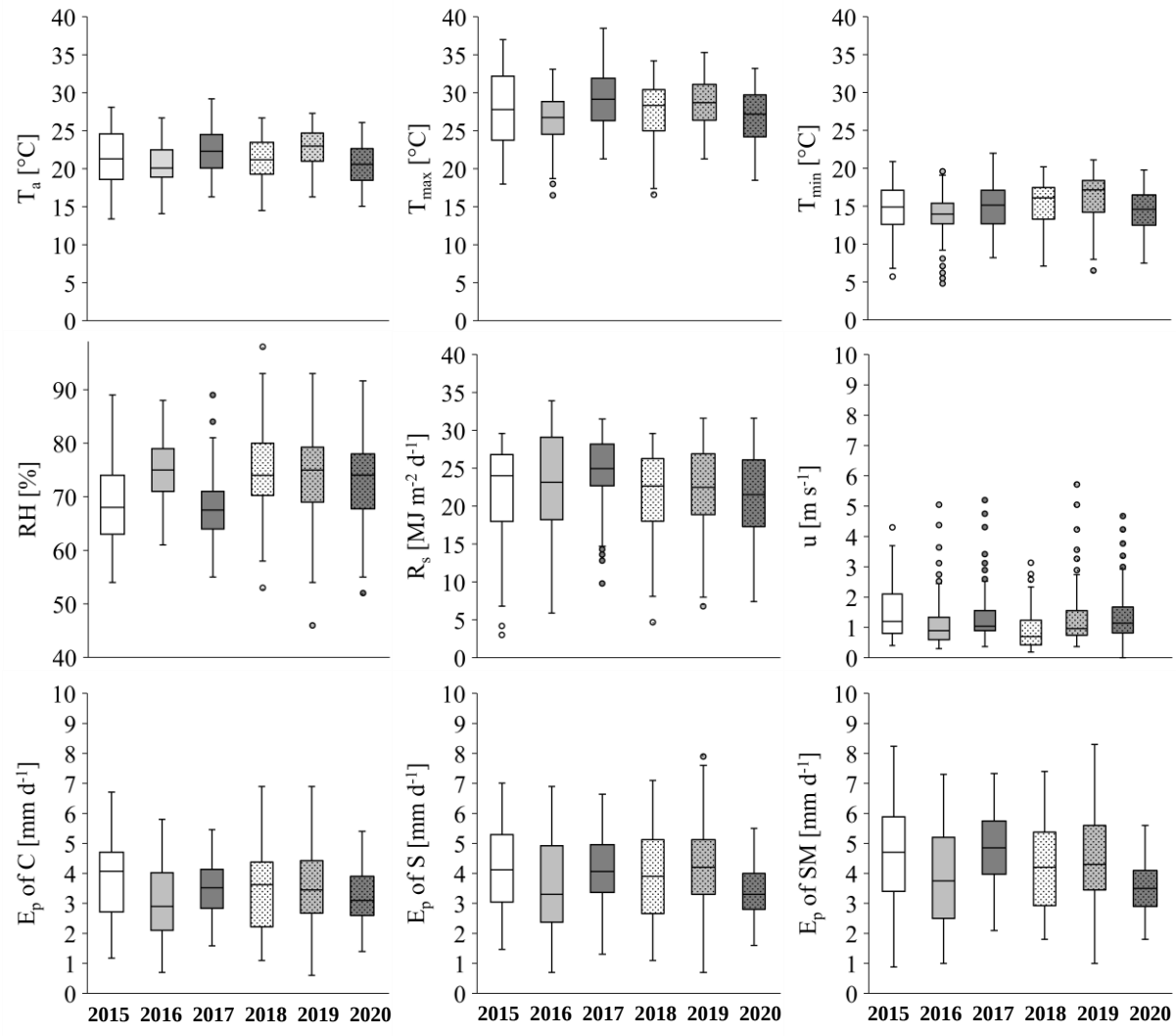

Figure 4: Box plot of meteorological parameters (T_a – daily mean temperature [°C], T_{max} – daily maximum temperature [°C], T_{min} – daily minimum temperature [°C], RH – relative humidity [%], R_s – global radiation [MJ m^{-2} d^{-1}], u – wind speed [m s^{-1}]) and daily evaporation of different pan treatments [mm d^{-1}] (C – control, S – Class A pan with sediment cover bottom, SM – Class A pan with submerged macrophyte) in 2015-2020 growing seasons (June-September).

Daily E_p rates were related to seasonal T_a variations and not to rainfall patterns. Average daily E_p varied from 0.6 to 6.9 mm d^{-1} for C, 0.7 to 7.9 mm d^{-1} for S, and from 0.9 to 8.2 mm d^{-1} for SM during the growing seasons studied. During the warmer seasons of 2015, 2018 and 2019, 10.2%, 10.1% and 7.8%higher daily mean E_p rates for C, S and SM, respectively, were recorded, compared to cooler growing seasons (Figure 4). A two-way ANOVA was conducted to explore the impact of the

https://doi.org/10.5194/hess-2021-590
Preprint. Discussion started: 1 December 2021

Hydrology and Earth System Sciences
Discussions

studied seasons and the treatment on E_p rates. There were significant main effects caused by the growing season ($F(5, 211) = 24.241$, $p = 0.001$) and the pan treatment ($F(2, 236) = 67.855$, $p = 0.001$) in full dataset. The interaction between seasons and treatments was not significant ($F(10, 29) = 0.085$, $p = 0.503$). Tukey HSD post-hoc tests revealed significant differences among the three pan treatments ($p < 0.001$ for all pairwise comparisons) for the training, testing phase and full dataset (Table 1).

Table 1. The impact of sediment (S) and submerged aquatic macrophytes (SM) on evaporation rates (E_p) of Class A pan (C) in the full data set (2015-2020), training (2015-2017) and testing (2018-2020) phase with 95% confidence intervals

Multiple Comparisons						
					95% Confidence Interval	
(I) treatment	(J) treatment	Mean difference (I-J)	Std. Error	Sig.	Lower Bound	Upper Bound
Full dataset (2015-2020)						
C	S	-0.490*	0.0733	**0.000**	-0.662	-0.318
	SM	-0.845*	0.0735	**0.000**	-1.017	-0.672
S	C	0.490*	0.0733	**0.000**	0.318	0.662
	SM	-0.355*	0.0733	**0.000**	-0.526	-0.183
SM	C	0.845*	0.0735	**0.000**	0.672	1.017
	S	0.355*	0.0733	**0.000**	0.183	0.526
Training data set (2015-2017)						
C	S	-0.712*	0.1066	**0.000**	-0.962	-0.462
	SM	-0.731*	0.1072	**0.000**	-0.982	-0.479
S	C	0.712*	0.1066	**0.000**	0.462	0.962
	SM	-0.019*	0.1124	**0.019**	-0.283	0.245
SM	C	0.731*	0.1072	**0.000**	0.479	0.982
	S	0.019*	0.1124	**0.019**	-0.245	0.283
Testing data set (2018-2020)						
C	S	-0.505*	0.0993	**0.000**	-0.738	-0.272
	SM	-0.716*	0.1001	**0.000**	-0.951	-0.481
S	C	0.505*	0.0993	**0.000**	0.272	0.738
	SM	-0.211*	0.0990	**0.045**	-0.443	0.022
SM	C	0.716*	0.1001	**0.000**	0.481	0.951
	S	0.211*	0.0990	**0.045**	-0.022	0.443

Based on observed means. The error term is Mean Square (Error) = 1.741.
Based on observed means. The error term is Mean Square (Error) = 1.840.
Based on observed means. The error term is Mean Square (Error) = 1.647.
*The mean difference is significant at the 0.05 level.

https://doi.org/10.5194/hess-2021-590
Preprint. Discussion started: 1 December 2021

Hydrology and Earth System Sciences
Discussions

The correlation of evaporation of different pan treatments with other meteorological variables is also given in Table 2. The T_a, T_{max} and R_s positively impacted the E_p, while RH had a negative correlation with E_p. In this study, u hardly affected the E_p rates irrespective to treatment. The descriptive statistics of both training and testing datasets showed that most of the meteorological variables and E_p were similar to the full data set.

Table 2. Statistics of meteorological variables (T_a - mean air temperature, T_{max} - maximum air temperature, T_{min} - minimum air temperature, RH - relative humidity, R_s - solar radiation, u - wind speed) and their correlation with evaporation (E_p) of C, S and SM in the full time series (2015-2020), training (2015-2017) and testing phases (2018-2020). C, S and SM are control class A pan, A pan with sediment cover-bottom and A pan with planted freshwater submerged macrophyte, respectively.

Data set	**Statistics**	**T_a** [°C]	**T_{max}** [°C]	**T_{min}** [°C]	**RH** [%]	**u** [m s^{-1}]	**R_s** [MJ m^{-2} day^{-1}]	**E_p of C** [mm d^{-1}]	**E_p of S** [mm d^{-1}]	**E_p of SM** [mm d^{-1}]
Full (2015-2020)	Average	21.1	27.5	14.8	72.7	1.3	22.4	3.4	3.9	4.3
	SD	3.2	4.0	3.2	8.0	0.9	6.0	1.2	1.4	1.5
	CV	0.15	0.14	0.21	0.11	0.70	0.27	0.35	0.35	0.35
	Max	29.2	38.5	22.0	98.0	5.7	33.9	6.9	7.9	8.3
	Min	11.7	16.5	4.8	46.0	0.0	3.0	0.6	0.7	0.9
	Correlation with E_p of C	0.59**	0.53**	0.42**	-0.43**	0.01	0.50**	1.00	-	-
	Correlation with E_p of S	0.57**	0.51**	0.40**	-0.42**	0.03	0.53**	0.92**	1.00	-
	Correlation with E_p of SM	0.56**	0.50**	0.37**	-0.44**	0.01	0.52**	0.90**	0.93**	1.00
Training (2015-2017)	Average	20.9	27.5	14.4	71.0	1.4	23.1	3.4	4.0	4.4
	SD	3.4	4.4	3.3	7.5	0.9	6.1	1.2	1.4	1.6
	CV	0.16	0.16	0.23	0.11	0.67	0.26	0.36	0.35	0.36
	Max	29.2	38.5	22.0	89.0	5.2	33.9	6.7	7.0	8.2
	Min	11.7	16.5	4.8	54.0	0.3	3.0	0.7	0.7	0.9
	Correlation with E_p of C	0.65**	0.59**	0.49**	-0.48**	0.05	0.51**	1.00	-	-
	Correlation with E_p of S	0.63**	0.58**	0.45**	-0.47**	0.00	0.56**	0.91**	1.00	-
	Correlation with E_p of SM	0.63**	0.57**	0.44**	-0.50**	0.04	0.54**	0.89**	0.93**	1.00
Testing	Average	21.2	27.4	15.3	74.2	1.2	21.8	3.4	3.9	4.1

https://doi.org/10.5194/hess-2021-590
Preprint. Discussion started: 1 December 2021


Hydrology and Earth System Sciences
Discussions

(2018-2020)	SD	2.9	3.5	3.0	8.2	0.9	5.7	1.2	1.4	1.4
	CV	0.13	0.13	0.20	0.11	0.73	0.26	0.35	0.35	0.34
	Max	27.3	35.3	21.1	98.0	5.7	31.6	6.9	7.9	8.3
	Min	12.1	16.6	6.5	46.0	0.0	4.7	0.6	0.7	1.0
	Correlation with E_p of C	0.53**	0.46**	0.35**	-0.41**	0.06	0.51**	1.00	-	-
	Correlation with E_p of S	0.51**	0.44**	0.35**	-0.39**	0.06	0.50**	0.92**	1.00	-
	Correlation with E_p of SM	0.49**	0.41**	0.33**	-0.38**	0.05	0.49**	0.92**	0.95**	1.00

**. Correlation is significant at the 0.01 level (2-tailed).

*. Correlation is significant at the 0.05 level (2-tailed).

3.2 K-SOM features

Two indicators are most often used to qualitatively evaluate the two main goals of the K-SOM algorithm: quantization error (QE) and topographic error (TE) (Table 3). The QE shows how closely the map vectors match the data vectors, thereby quantifying map resolution (Kohonen, 1995). The TE, in turn, determines the extent to which the topology of the input data structure is preserved on the output map (Kiviluoto, 1996). QE and TE does not have a default value, but the smaller the QE and TE (if the values tend to be zero) the better the model is. In this study, the values of QE and TE were equal to 0.016 and 0.820, respectively, indicating that the K-SOM was appropriately trained in topology.

Table 3 Characteristics of trained Kohonen Self-Organizing Map (K-SOM) model

Characteristics	**Values**
Normalization method	variance: $x' = (x - \bar{x})/\sigma_x$
Codebook	312 x 3
Map Size	24 x 13
Neighbourhood function	Gaussian
Shape	Sheet
Lattice	Hexagonal
Final Topographic error (TE)	0.820
Final Quantization error (QE)	0.016

K-SOM can be interpreted using the output map and the individual component planes, so the relationships between each variable can be explored. The component planes help to visually illustrate areas in which the intensity of the relationship of

https://doi.org/10.5194/hess-2021-590
Preprint. Discussion started: 1 December 2021

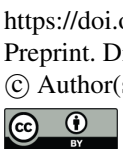

Hydrology and Earth System Sciences
Discussions

the variables is high, low, or average and thus helps to better understand the relationship between the E_p and meteorological variables. The component planes for each variable of the K-SOM model are shown in Figure 5.

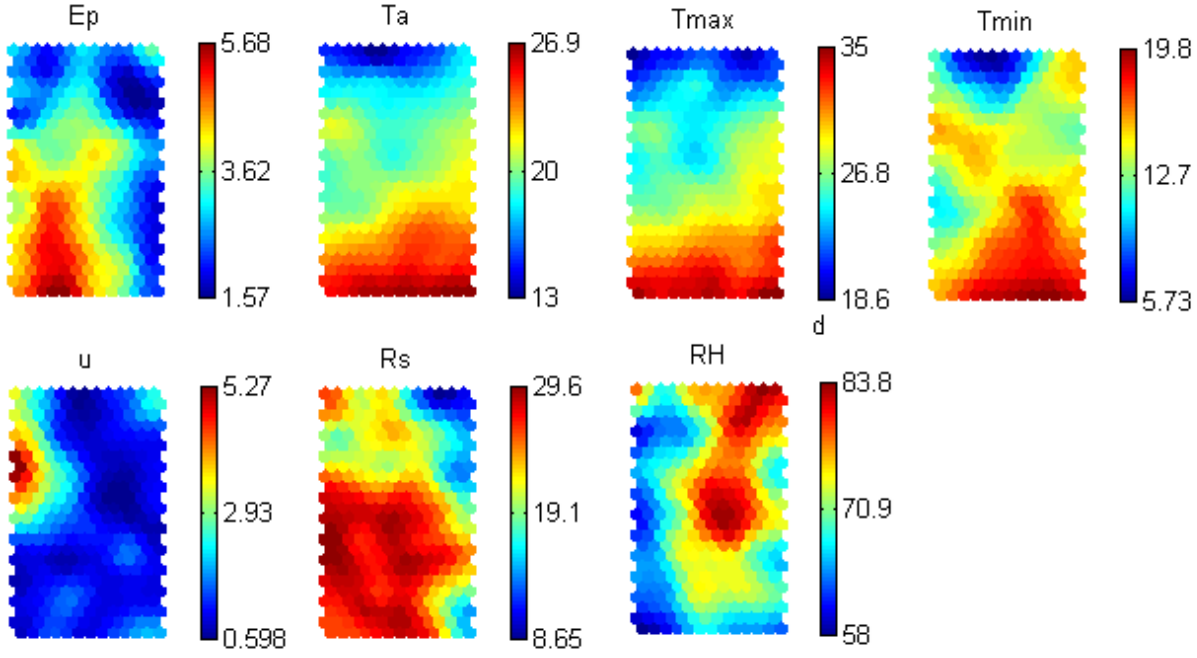

Figure 5: Kohonen Self-Organizing Map (K-SOM) visualization of pan evaporation and meteorological variables assessment (T_a – daily mean temperature [°C], T_{max} – daily maximum temperature [°C], T_{min} – daily minimum temperature [°C], RH – relative humidity [%], R_s – global radiation [MJ m^{-2} d^{-1}], u – wind speed [m s^{-1}] and E_p - daily evaporation [mm d^{-1}]). The bars indicate the intensity of the variables: the red colour is high importance, and the blue colour is low importance.

On the maps, the warm colours (red, orange) show positive correlation between the study variables, and the darker the colours (blue), the lower the relative value of the component of the corresponding variable. Thus, the correlation between the K-SOM modelled values of E_p, T_a, T_{min}, T_{max}, R_s, RH, and u becomes clearly visible. The colour gradient of E_p was similar to those for variables related to available energy (T_a, T_{min}, T_{max} and R_s), indicating that these contribute most to the increase of E_p. The component planes also visually confirm the negative correlation between RH and E_p, with high values of the RH resulting in low values of the E_p.

3.3 FAO56-PM, MLR and K-SOM models

Figure 6. depicts the time variation and X-Y scatter plots of the observed and estimated daily E_p values obtained by C, S and SM during the testing period (2018-2020).

https://doi.org/10.5194/hess-2021-590
Preprint. Discussion started: 1 December 2021

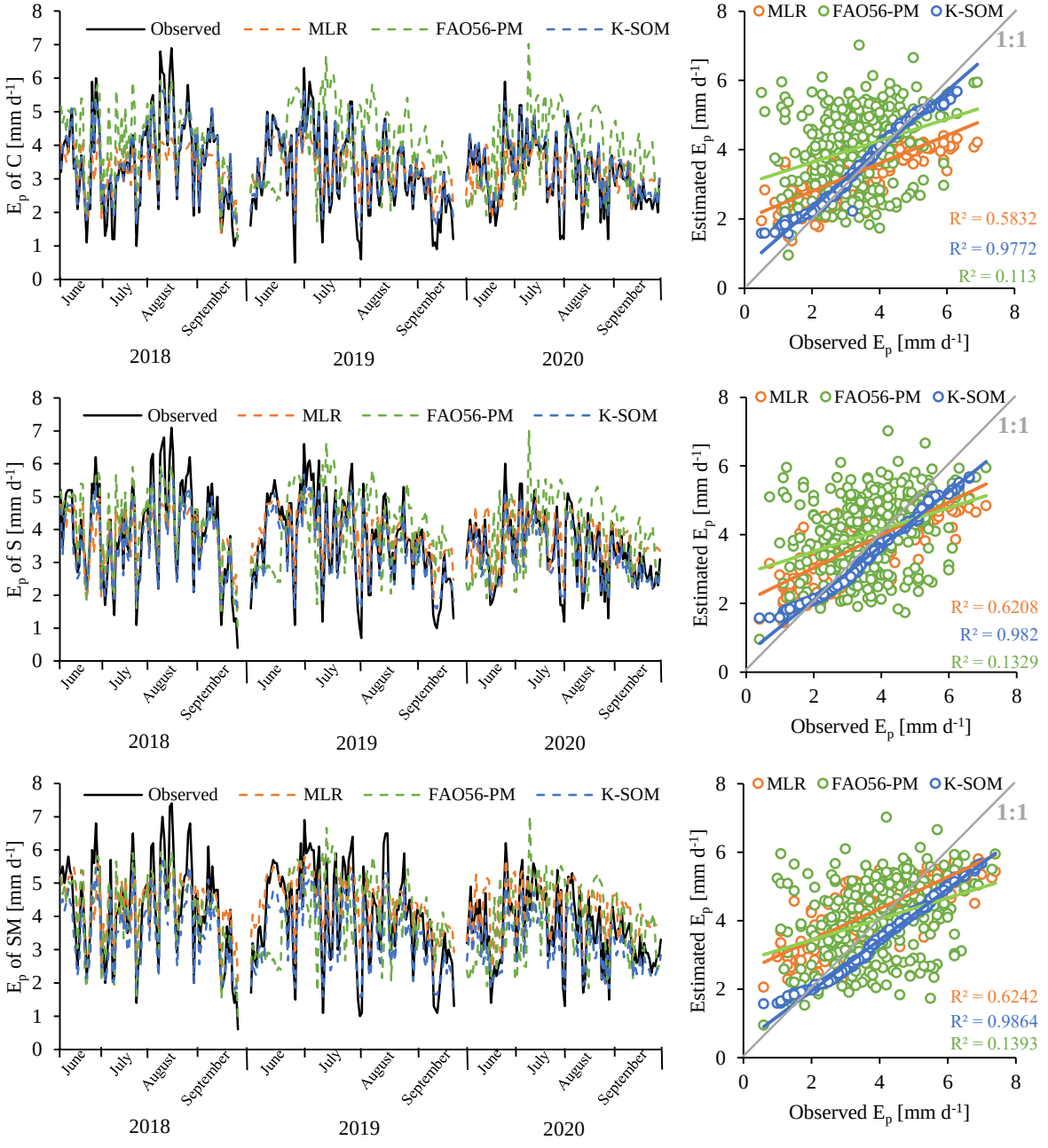

Figure 6: Time series and X-Y scatter plot of observed and predicted daily pan evaporation (E_p) in different pan treatment (C – control, S – pan with sediment cover bottom, SM – pan with submerged macrophytes) by daily multiple stepwise regression (MLR), FAO-56 Penman-Monteith (FAO56-PM) and Kohonen self-organization map (K-SOM) models during testing period (2018-2020 growing seasons).

From the figure, it can be observed that most of the estimated daily E_p values are close to the observed daily E_p values for all three pan treatments. The regression line is above the 1:1 line up to 4 mm, which means that the FAO56-PM and MLR models

https://doi.org/10.5194/hess-2021-590
Preprint. Discussion started: 1 December 2021

Hydrology and Earth System Sciences
Discussions

slightly overestimated the magnitude of the daily E_p values in different pan treatments. However, above 4 mm daily E_p, the FAO56-PM and MLR models already underestimated the observed E_p values. The daily E_p values of C, S, and SM of the K-SOM model follow the 1:1 line most accurately. For all three models, R2 values were highest for MS treatment (FAO56-PM: 0.1393, MLR: 0.6242, K-SOM: 9864). In the case of K-SOM, it can also be observed that low E_p values are overestimated, while higher E_p values are underestimated, although the estimated "middle" E_p values (which occur most frequently in a growing season) were close to the observed E_p values regardless of pan treatment. A greater degree of underestimation is observed for MS treatment for K-SOM.

4 Discussion

To date, there is few information about the impact of submerged aquatic macrophytes on E_p rate. According to a previous study, aquatic plants evapotranspirated 26% more water than free water surface (Brezny et al., 1973). Anda et al. (2016; 2018) have shown that the presence of sediment increases the evaporation of the Class A pans by an average of 12.7% and the submerged aquatic macrophytes by an average of 21.3%. Jiménez-Rodríguez et al., (2019) reported that the observed E_p were higher for aquatic plants than the open water cover. Concerning the relationship between pan treatments and meteorological variables, it can be concluded that positive correlation was observed with most meteorological variables, while a negative correlation was observed with RH. This result was supported by other researches in the literature (Sheffield et al., 2017). In this study, u hardly affected the E_p rates of each treatment. This does not confirm the conclusions made by earlier studies (McVicar et al., 2012). This may be due to the fact that Keszthely is sheltered by surrounding mountains causing lower wind speeds (Anda et al., 2016).

In this study, we developed E_p models based on three different approaches (FAO56-PM, MLR and K-SOM) with daily meteorological variables, and tested the performance of the models by four commonly used statistical indicators (MAE [Ideal = 0, (0,+∞)], RMSE [Ideal = 0, (0,+∞)], NSE [Ideal = 1, (−∞,1)], SI [Ideal = 0, (0,+∞)]). Figure 7 shows the overall performance of the three predicted methods at the three pan treatments.

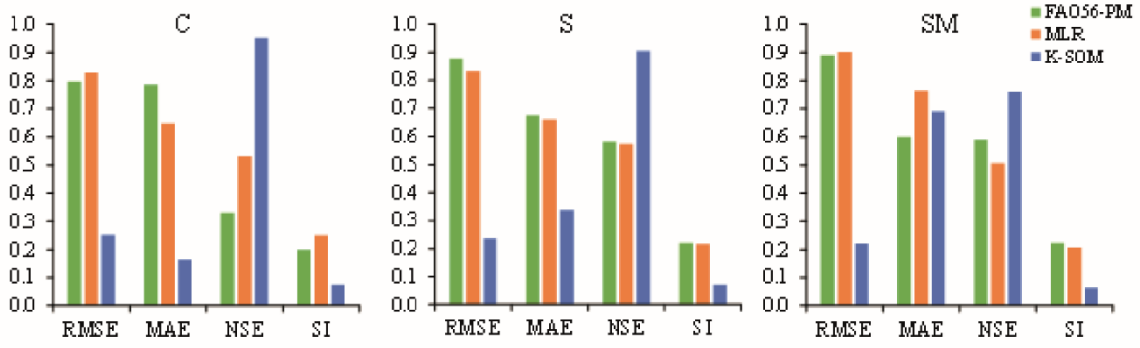

Figure 7: Error statistics (root mean square error - RMSE, mean absolute error - MAE, scatter index - SI and Nash-Sutcliffe efficiency - NSE) for the multiple stepwise regression (MLR), FAO-56 Penman-Monteith reference crop evapotranspiration (FAO56-PM) and Kohonen self-organization map (K-SOM) models during the testing period for different pan treatments (C is

https://doi.org/10.5194/hess-2021-590
Preprint. Discussion started: 1 December 2021


Hydrology and Earth System Sciences
Discussions

standard class A pan with clean water, S is class A pan with sediment cover bottom, and SM is class A pan containing submerges macrophyte).

The K-SOM models (RMSE = 0.222–0.253; NSE = 0.761–0.951; SI = 0.065–0.074) performed the best in the testing period, and their RMSE and MAPE were lower, and their NSE were higher than those of FAO56-PM and MLR models regardless of pan treatment (C: 0.951; S: 0.906; SM: 0.761). Additionally, the MAE value for treatments C and S was the lowest in the K-SOM models (MAE = 0.164 and MAE = 0.338, respectively), in contrast, the FAO56-PM had the best MAE value for SM treatment (MAE=0.601).

Overall, the MLR (RMSE = 0.834; MAE = 0.660; S = 0.217) was slightly superior to FAO56-PM (RMSE = 0.877; MAE = 0.675; SI = 0.220) in the S, and there was only a small difference in the value of NSE between the two models (MLR: 0.572; FAO56-PM: 0.580). In the C treatment, RMSE (0.796) and SI (0.200) were lower for FAO56-PM, while MAE (0.648) and NSE (0.531) values were more favourable for the MLR model. Nevertheless, both the K-SOM model and MLR model were better than the FAO56-PM model during the testing period for "non-empty" treatments (S and SM).

Many researchers have conducted research with neural networks aimed at the estimation of E_p as a function of meteorological variables (Keskin and Terzi, 2006). Several of these researchers found better results in E_p estimation with neural network than those obtained from the Priestley-Taylor and the Penman methods (Rahimikhoob, 2009; Malik et al., 2020). Consistent with other studies, this study demonstrated that modelling of E_p is possible through the use of K-SOM technique in addition to the FAO56-PM and MLR methods. The comparison results indicated that, in general, the K-SOM model was superior to the FAO56-PM and MLR methods. Chang et al. (2010) used different methods to estimate pan evaporation, including also the K-SOM and the FAO56-PM. According to the results of Chang et al. (2010), K-SOM was the best of the studied methods, and it was found that the Penman-Monteith method is also likely to underestimate evaporation. Malik et al. (2017) used four heuristic approaches and two climate-based models to approximate monthly pan evaporation, where the K-SOM model performed better than the climate-based models. The regression line in scatter plots has R^2 as 0.937 for K-SOM model at Pantnagar and Ranichauri (India), respectively. In the study of Malik et al. (2017), RMSE values were 0.685 and 1.126 for K-SOM, when 50% of the total available data was used in the testing of models in two stations.

4 Conclusions

The E_p of a class A pan with submerged aquatic macrophytes and with a sediment-covered bottom was observed at Keszthely, over six consecutive (2015-2020) growing seasons. In this study, it was attempted to model E_p by employing models consisting of FAO56-PM, MLR and K-SOM, using daily pan evaporation values in different Class A pan treatments (C, S, SM). The E_p rate of SM and S was always significantly higher than that of the "empty" class A pan each growing season. The presence of submerged macrophyte resulted in a higher E_p than in the sediment-covered class A pan.

Daily E_p rates for all pan treatments were related to seasonal T_a variations. Correlation analysis revealed that T_a, T_{max}, T_{min} and R_s had a positive correlation with pan evaporation, whereas RH had a negative correlation (-0.42-0.44) with E_p of C, S and

https://doi.org/10.5194/hess-2021-590
Preprint. Discussion started: 1 December 2021


Hydrology and Earth System Sciences
Discussions

SM in full dataset. Among all, the R of T_a (ranged from 0.56-0.59) had a stronger positive correlation followed by R of T_{max} (ranged from 0.50-0.53) and R of R_s (ranged from 0.50-0.53). The relationship with u was low for the E_p of the three treatments, which can be explained by the low u of Keszthely in the growing seasons. Using the visualization capability of the K-SOM, it was clearly confirmed that the E_p was more closely correlated with the variables related to available energy, than the RH.

The performance accuracy of the different applied models was evaluated with RMSE, MAE, NSE and SI statistics. Results showed that the K-SOM model has high priority in prediction precision over the FAO56-PM and MLR models. Comparing the FAO56-PM and MLR models, MLR performed better in this study in S and SM treatments.

Hydrometeorological networks and water resource management can obtain useful information from the results of the current research. The findings of this specific study should also be investigated further in correlation with different neural network methods and different climate types in the future.

Acknowledgements

Project PD_21 was implemented with the support of the Ministry for Innovation and Technology from the Source of the National Research, Development and Innovation Fund, in the financing of the PD 138660 application program. Supported by the ÚNKP-20-4-II New National Excellence Program of the Ministry for Innovation and Technology from the Source of the National Research, Development and Innovation Fund.

References

Adeloye, A. J., Rustum, R. and Kariyama, I.D.: Kohonen self-organizing map estimator for the reference crop evapotranspiration, Water Resour. Res., 47, W08523, doi:10.1029/2011WR010690, 2005.

Allen, R. G., Pereira, L. S., Raes, D. and Smith, M.: Crop Evapotranspiration: Guidelines for Computing Crop Water Requirements, Irrigation and Drainage Paper 56, Food and Agriculture Organization of the United Nations: Rome, Italy. http://www.fao.org/3/x0490e/x0490e00.htm, 1998.

Allen, R. G., Walter, I. A., Elliott, R., Howell, T., Itenfisu, D., Jensen, M., and Synder, R. L.: The ASCE Standardized Reference Evapotranspiration Equation, Final Report (ASCE–EWRI), Task Committee on Standardization of Reference Evapotranspiration, Environmental and Water Resources Institute of the American Society of Civil Engineers: Reston, VA, USA, doi:10.1061/9780784408056, 2005.

Almedeij, J.: Modeling pan evaporation for Kuwait by multiple linear regression, Sci. World J., 2012, 574742, doi: 10.1100/2012/574742, 2012.

An, N., Wang, K., Zhou, C. and Pinker, R. T.: Observed variability of cloud frequency and cloud-based height within 3600 m above the surface over the contiguous United States, J. Climate, 30, 3725–3742, doi:10.1175/JCLI-D-16-0559.1, 2017.

320 Anda, A., Simon, B., Soós, G., Menyhárt, L., Teixeira da Silva, J. A. and Kucserka, T.: Extending Class A pan evaporation for a shallow lake to simulate the impact of littoral sediment and submerged macrophytes: a case study for Keszthely Bay (Lake Balaton, Hungary), Agr. Forest Meteorol., 250–251, 277-289, doi:10.1016/j.agrformet.2018.01.001, 2018

Anda, A., Simon, B., Soos, G., Teixeira da Silva, J. A. and Kucserka, T.: Effect of submerged, freshwater aquatic macrohytes and littoral sediments on pan evaporation in the Lake Balaton region, Hungary, J. Hydrol., 542, 615–626,
325 doi:10.1016/j.jhydrol.2016.09.034, 2016.

Arunkumar, R. and Jothiprakash, V.: Reservoir evaporation prediction using data driven techniques, J. Hydrol. Eng., 18(1), 40–49, doi:10.1061/(ASCE)HE.1943-5584.0000597, 2013.

ASCE Task Committee on Definition of Criteria for Evaluation of Watershed Models: Criteria for evaluation of watershed models, J. Irrig. Drain. Eng., 119(3), 429–442, doi:10.1061/(ASCE)0733-9437(1993)119:3(429), 1993.

330 Barko, J. W., Hardin, D. G. and Matthews, M. S.: Growth and morphology of submersed freshwater macrophytes in relation to light and temperature, Can. J. Botany, 60(6), 877–887, doi:10.1139/b82-113, 1982

Barreto, S. M. A. and Pérez-Uribe, A.: Improving the Correlation Hunting in a Large Quantity of SOM Component Planes. In: de Sá, J. M., Alexandre, L. A., Duch, W. and Mandic, D. (eds): Artificial Neural Networks – ICANN 2007. Lect. Notes Comput. Sc., 4669. Springer, Berlin, Heidelberg, 379–388 pp, doi:10.1007/978-3-540-74695-9_39, 2007.

335 Brezny, O., Mehta, I. and Sharmas, R. K.: 1973. Studies of evapotranspiration of some aquatic weeds, Weed Sci., 21(3), 197–204, doi:10.1017/S0043174500032112, 1973.

Brutsaert, W. H.: 1982. Evaporation into the Atmosphere, Springer, 12–36 pp, doi:10.1007/978-94-017-1497-6, 1982.

Burman, R. D.: Intercontinental comparison of evaporation estimates, J. Irr. Drain. Div.-ASCE, 102(1), 109–118, doi:10.1061/JRCEA4.0001076, 1976.

340 Chang, F. J., Chang, L. C., Kao, H. S. and Wu, G. R.: Assessing the effort of meteorological variables for evaporation estimation by self-organizing map neural network, J. Hydrol., 384, 118–129, doi:10.1016/j.jhydrol.2010.01.016, 2010.

Dong, L., Zeng, W., Wu, L., Lei, G., Chen, H., Srivastava, A. K. and Gaiser, T.: Estimating the pan evaporation in Northwest China by coupling CatBoost with Bat algorithm, Water, 13, 256, doi:10.3390/w13030256, 2021.

Duan, W. Y., Han, Y., Huang, L. M., Zhao, B. B. and Wang, M. H.: A hybrid EMD-SVR model for the short-term prediction
345 of significant wave height, Ocean Eng., 124, 54–73, doi:10.1016/j.oceaneng.2016.05.049, 2016.

Fournier, J., Thiboult, A., Nadeau, D. F., Vercauteren, N., Anctil, F., Parent, A.-C., Strachan, I. B. and Tremblay A.: Evaporation from boreal reservoirs: Acomparison between eddy covariance observations andestimates relying on limited data, Hydrol. Process., 35(8), e14335, doi:10.1002/hyp.14335, 2021.

Hadjisolomou, E., Stefanidis, K., Papatheodorou, G. and Papastergiadou, E.: Assessment of the eutrophication-related
350 environmental parameters in two mediterranean lakes by integrating statistical techniques and self-organizing maps, Int. J. Env. Res. Pub. He., 15, 547, doi:10.3390/ijerph15030547, 2018.

Jensen, M. E., Burman, R. D. and Allen, R. G.: Evapotranspiration and irrigation water requirements, American Society of Civil Engineers 70, New York, 332 pp, doi:10.1061/9780784414057, 1990.

https://doi.org/10.5194/hess-2021-590
Preprint. Discussion started: 1 December 2021


Hydrology and Earth System Sciences
Discussions

Jiménez-Rodríguez, C. D., Esquivel-Vargas, C., Coenders-Gerrits, M. and Sasa-Marín, M.: Quantification of the Evaporation Rates from Six Types of Wetland Cover in Palo Verde National Park, Costa Rica, Water, 11(4), 674, doi:10.3390/w11040674, 2019.

Keskin, M. E. and Terzi, O.: Artificial neural network models of daily pan evaporation, J. Irrig. Drain. Eng., 11(1), 65–70, doi:10.1061/(ASCE)1084-0699(2006)11:1(65), 2006.

Khatibi, R., Ghorbani, M. A., Naghshara, S., Aydin, H. and Karimi, V.: Introducing a framework for 'inclusive multiple modelling' with critical views on modelling practices-Applications to modelling water levels of Caspian Sea and Lakes Urmia and Van, J. Hydrol., 587, 124923, doi:10.1016/j.jhydrol.2020.124923, 2020.

Kim, S., Shiri, J., Singh, V. P., Kisi, O. and Landeras, G.: Predicting daily pan evaporation by soft computing models with limited climatic data, Hydrolog. Sci. J., 60(6), 1120–1136, doi:10.1080/02626667.2014.945937, 2015.

Kimmel, B. L. and Groeger, A. W.: Factors controlling primary production in lakes and reservoirs: a perspective, Lake Reserv. Manage., 1, 277–281, doi:10.1080/07438148409354524, 1984.

Kiviluoto, K.: Topology preservation in self-organizing maps, Proceedings of International Conference on Neural Networks, 294–299, doi:10.1109/ICNN.1996.548907, 1996.

Kohonen, T.: Self-organizing formation of topologically correct feature maps, Biol. Cybern., 43, 59–69, doi:10.1007/BF00337288, 1982.

Kottek, M., Grieser, J., Beck, C., Rudolf, B. and Rubel, F.: WorldMap of the Köppen-Geiger climate classification updated, Meteorologische Zeitschrift, 15(3), 259–263, doi:10.1127/0941-2948/2006/0130, 2006.

Kumar, M., Raghuwanshi, N. S., Singh, R., Wallender, W. W. and Pruitt, W. O.: Estimating evapotranspiration using artificial neural network, J. Irrig. Drai. Eng., 128(4), 224–233, doi:10.1061/(ASCE)0733-9437(2002)128:4(224), 2002.

Li, M. and Liu, K.: Probabilistic prediction of significant wave height using dynamic bayesian network and information flow, Water, 12, 2075, doi:10.3390/w12082075, 2020.

Madsen, T. V. and Cedergreen, N.: Sources of nutrients to rooted submerged macrophytes growing in a nutrient-rich stream, Freshwater Biol., 47, 283–291, doi:10.1046/j.1365-2427.2002.00802.x, 2002.

Malik, A., Kumar, A. and Kisi, O.: Monthly pan-evaporation estimation in Indian central Himalayas using different heuristic approaches and climate based models, Comput. Electron. Agr., 143, 302–313, doi:10.1016/j.compag.2017.11.008, 2017.

Malik, A., Rai, P., Heddam, S., Kisi, O., Sharafati, A., Salih, S. Q., Al-Ansari, N. and Yaseen, Z. M.: Pan evaporation estimation in Uttarakhand and Uttar Pradesh States, India: validity of an integrative data intelligence model, Atmosphere, 11, 553, doi:10.3390/atmos11060553, 2020.

Mbangiwa, N. C., Savage, M. J. and Mabhaudhi, T.: Modelling and measurement of water productivity and total evaporation in a dryland soybean crop, Agric. For. Meteorol., 266–267, 65–72, doi:10.1016/j.agrformet.2018.12.005, 2019.

McVicar ,T. R., Roderick, M. L., Donohue, R. J., Li, L. T., van Niel, T. G., Thomas, A., Grieser, J., Jhajharia, D., Himri, Y., Mahowald, N. M., Mescherskaya, A. V., Kruger, A. C., Rehman, S. and Dinpashohl, Y.: Global review and synthesis of trends

in observed terrestrial near-surface wind speeds: implications for evaporation, J. Hydrol., 416–417, 182–205, doi:10.1016/j.jhydrol.2011.10.024, 2012.

Nash, J. E. and Sutcliffe, J. V.: River flow forecasting through conceptual models part I — a discussion of principles, J. Hydrol., 10(3), 282–290, doi:10.1016/0022-1694(70) 90255-6, 1970.

Park, Y. S., Lek, S., Scardi, M., Verdonschot, P. and Jorgensen, S. E.: Patterning exergy of benthic macroinvertebrate communities using self-organizing maps, Ecol. Model., 195(1), 105–113 doi:10.1016/j.ecolmodel.2005.11.027, 2006.

Patle, G. T., Chettri, M. and Jhajharia, D.: Monthly pan evaporation modelling using multiple linear regression and artificial neural network techniques, Water Supply, 20(3), 800–808, doi:10.2166/ws.2019.189, 2020.

Pearce, A. R., Rizzo, D. M. and Mouser, P. J.: Subsurface characterization of groundwater contaminated by landfill leachate using microbial community profile data and a nonparametric decision-making process, Water Resour. Res., 47, W06511, doi:10.1029/2010WR009992, 2011.

Peeters. L., Bacao, F., Lobo, V. and Dassargues, A.: Exploratory data analysis and clustering of multivariate spatial hydrogeological data by means of GEO3DSOM, a variant of Kohonen's Self-Organizing Map, Hydrol. Earth Syst. Sc., 11, 1309–1321, doi:10.5194/hess-11-1309-2007, 2007.

Rahimikhoob, A.: Estimating daily pan evaporation using artificial neural network in a semi-arid environment, Theor. Appl. Climatol., 98, 101–105, doi:10.1007/s00704-008-0096-3, 2009.

Razi, M. A. and Athappilly, K.: A comparative predictive analysis of neural networks (NNs), nonlinear regression and classification and regression tree (CART) models, Expert Syst. Appl., 29(1), 65–74, doi:10.1016/j.eswa.2005.01.006, 2005.

Sanikhani, H., Kisi, O., Kiafar, H. and Ghavidel, S. Z. Z.: Comparison of different data-driven approaches for modeling lake level fluctuations: the case of Manyas and Tuz Lakes (Turkey). Water Resour. Manag., 29(5), 1557–1574, doi:10.1007/s11269-014-0894-6, 2015.

Sheffield, J., Goteti, G. and Wood, E. F.:. Development of a 50-Year high-resolution global dataset of meteorological forcings for land surface modelling, J. Climate, 19, 3088–3111, doi:10.1175/JCLI3790.1, 2006.

Shiri, J. and Kisi, O.: Application of artificial intelligence to estimate daily pan evaporation using available and estimated climatic data in the Khozestan Province (South-Western Iran), J. Irrig. Drain. Eng., 137(7), 412–425, doi:10.1061/(ASCE)IR.1943-4774.0000315, 2011.

Sudheer, K. P., Gosain, A. K. and Ramasastri, K. S.: Estimating actual evapotranspiration from limited climatic data using neural computing technique, J. Irrig. Drain. Eng., 129(3), 214–218, doi:10.1061/(ASCE)0733-9437(2003)129:3(214), 2003.

Tabari, H., Marofi, S. and Sabziparvar, A. A.: Estimation of daily pan evaporation using artificial neural network and multivariate non-linear regression, Irrigation Sci, 28, 399–406, doi:10.1007/s00271-009-0201-0, 2010.

Vymazal, J.: Emergent plants used in free water surface constructed wetlands: a re-view, Ecol. Eng., 61B, 582–592, doi:10.1016/J.ECOLENG.2013.06.023, 2013.

Wu, L., Huang, G., Fan, J., Ma, X., Zhou, H. and Zeng, W.: Hybrid extreme learning machine with metaheuristic algorithms for monthly pan evaporation prediction, Comput. Electron. Agr., 168, 105115, doi:10.1016/j.compag.2019.105115, 2020.

https://doi.org/10.5194/hess-2021-590
Preprint. Discussion started: 1 December 2021


Hydrology and Earth System Sciences
Discussions

Yan, K., Yuan, Z., Goldberg, S., Gao, W., Ostermann, A., Xu, J., Zhang, F. and Elser, J.: Phosphorus mitigation remains critical in water protection: A review andmeta-analysis from one of China's most eutrophicated lakes, Sci. Total Environ., 689, 1336–1347, doi:10.1016/j.scitotenv.2019.06.302, 2019.

Yan, L., Mu, X., Han, B., Zhang, S., Qiu, C. and Ohore, O. E.: Ammonium loading disturbed the microbial food webs in biofilms attached to submersed macrophyte *Vallisneria natans*, Sci. Total Environ., 659, 691–698, doi:10.1016/j.scitotenv.2018.12.423, 2019.

Yu, Z. Q., Amano, H., Nakagawa, K. and Berndtsson, R.: Hydrogeochemical evolution of groundwater in a Quaternary sediment and Cretaceous sandstone unconfined aquifer in Northwestern China, Environ. Earth Sci., 77, 629, doi:10.1007/s12665-018-7816-5, 2018.

Zelazny, M., Astel, A., Wolanin, A. and Malek, S.: Spatiotemporal dynamics of spring and stream water chemistry in a high-mountain area, Environ. Pollut., 159, 1048–1057, doi:10.1016/j.envpol.2010.11.021, 2011.

Zhang, Y., Jeppesen, E., Liu, X., Qin, B., Shi, K., Zhou, Y., Thomaz, S. M. and Deng, J.: Global loss of aquatic vegetation in lakes, Earth-Sci. Rev., 173, 259–265, doi:10.1016/j.earscirev.2017.08.013, 2017.